

# Shape-dependent anisotropy and damping of picosecond magnetisation dynamics in a micron sized $\text{Ni}_{81}\text{Fe}_{19}$ element

A. Barman<sup>a,\*</sup>, V.V. Kruglyak<sup>a</sup>, R.J. Hicken<sup>a</sup>, A. Kundrotaitė<sup>b</sup>, M. Rahman<sup>b</sup>

<sup>a</sup>*School of Physics, University of Exeter, Stocker Road, Exeter EX4 4QL, UK*

<sup>b</sup>*Department of Physics and Astronomy, University of Glasgow, Glasgow G12 8QQ, UK*

## Abstract

We have observed a four-fold variation of the anisotropy and damping of the magnetisation precession in a square  $\text{Ni}_{81}\text{Fe}_{19}$  element of  $10\ \mu\text{m}$  length by time-resolved scanning Kerr-effect microscopy. The measured frequencies are interpreted with the aid of a coherent rotation model, while micromagnetic modelling is used to understand the dynamic magnetic images and hence the variation of the damping.

© 2004 Elsevier B.V. All rights reserved.

PACS: 78.47.+p; 76.50.+g; 85.70.kh

Keywords: Magnetic microscopy; Ultrafast magnetic processes; Magnetic thin film device

Time-resolved scanning Kerr-effect microscopy (TRSKEM) is a powerful probe of ultrafast magnetisation dynamics in small magnetic elements [1–3]. The dipolar interactions within the element depend upon its size and shape, give rise to configurational anisotropy [3–5], and influence the apparent damping [3]. In this article a four-fold dependence of anisotropy and damping is observed in a square element both experimentally and in micromagnetic simulations.

The sample is a square  $\text{Ni}_{81}\text{Fe}_{19}$  element of  $150\ \text{nm}$  thickness and  $10\ \mu\text{m}$  side fabricated on a glass substrate [3]. Hysteresis loops showed saturation fields of up to  $110\ \text{Oe}$ . A pulsed field  $\mathbf{h}(t)$ , with  $35\ \text{ps}$  rise time and  $27\ \text{Oe}$  peak height, and a static magnetic field  $\mathbf{H}$  with strength  $H$  and orientation  $\phi_H$  were applied within the plane of the sample. The p-polarised probe beam of  $800\ \text{nm}$  wavelength and  $120\ \text{fs}$  pulse-width was focused to a sub- $\mu\text{m}$  spot and the Kerr rotation of the back-reflected beam was recorded.

Fig. 1(a) shows the time-dependent Kerr rotation  $\theta_K$  measured at the centre of the sample for  $H = 410\ \text{Oe}$  and different values of  $\phi_H$  and the right-hand panel shows the fast Fourier transforms (FFT). The time scans

show that the damping has a four-fold dependence upon  $\phi_H$ . The FFTs show a prominent peak corresponding to the uniform mode of precession. The dependence of the peak position upon  $\phi_H$  is plotted in Fig. 2(a) and has four-fold symmetry. The uniform mode frequency has been modelled by inserting four-fold and uniaxial anisotropy terms into the solution of the Landau–Lifshitz equation [3,6]. The simulated frequencies, shown by the solid line in Fig. 2(a), agree with the experimental frequencies. Modelling yielded values of  $2$  and  $-33\ \text{Oe}$  for the uniaxial and four-fold anisotropy fields, and values of  $10.8\ \text{kOe}$  for  $4\pi M_S$  ( $M_S$  is the saturation magnetisation) and  $2.1$  for the  $g$  factor. Micromagnetic simulations were performed with the OOMMF software [7]. The element was divided into a 2D grid of  $40\ \text{nm}$  squares and a value of  $0.01$  was assumed for the damping coefficient. The time dependence of the out-of plane component of the magnetisation ( $M_Z$ ), averaged over the entire area of the element, is shown for various  $\phi_H$  values in Fig. 1(b) with corresponding FFT spectra. The simulated curves again show that the damping has a four-fold dependence.

The frequencies obtained from OOMMF are plotted as a function of  $\phi_H$  in Fig. 2(a). The widths of the FFT spectra provide a measure of the damping and are plotted in Fig. 2(b). The finite length of the time scan

\*Corresponding author. Tel.: +44-1392-264104; fax: +44-1392-264111.

E-mail address: [n.barman@exeter.ac.uk](mailto:n.barman@exeter.ac.uk) (A. Barman).

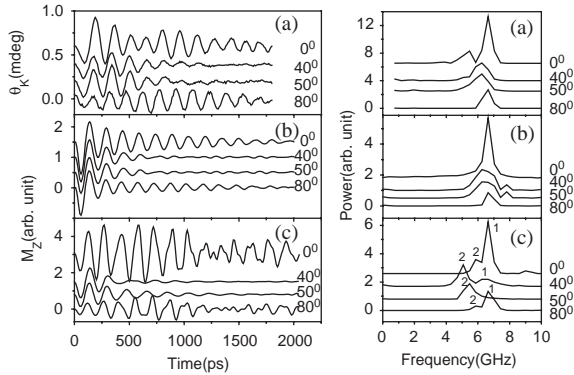


Fig. 1. (a) The measured Kerr rotation ( $\theta_K$ ) is plotted. Simulated  $M_Z$ , (b) averaged over the entire area of the sample, and (c) from a  $1 \mu\text{m}$  area at the centre of the sample, are shown. The right-hand panels show the corresponding FFT spectra.

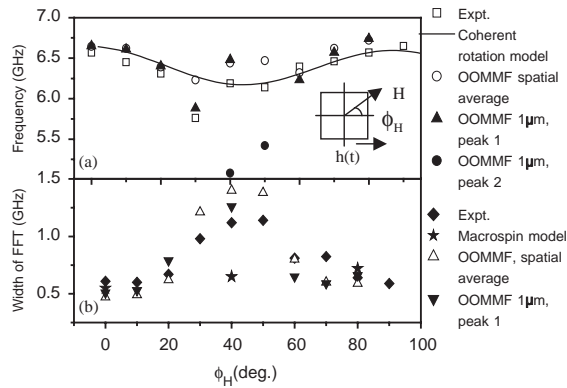


Fig. 2. (a) Frequencies and (b) widths of the FFT spectra are plotted as function of  $\phi_H$ . The inset in (a) shows the measurement geometry.

used in experiment and simulation contributes to about 30% of the width of the peak in the FFT. The simulated frequencies show a strong four-fold dependence and a weak eight-fold dependence that was observed before both experimentally and in micromagnetic simulations [5]. The measured and simulated linewidths follow a similar trend although the angular variation of the simulated linewidth is slightly stronger. The widths obtained from a macrospin model did not show any significant variation with  $\phi_H$ .

In order to reproduce the experimental conditions, the average  $M_Z$  value from a square of  $1 \mu\text{m}^2$  area at the centre of the element is plotted in Fig. 1(c). The FFTs show a lower frequency mode which has greater amplitude than the uniform mode when  $\phi_H = 40\text{--}50^\circ$ . This mode was not observed consistently in the experiment. This may explain why the damping is apparently stronger in Fig. 1(c) than in the experiment and suggests that a complete characterisation of the mode spectrum is needed.

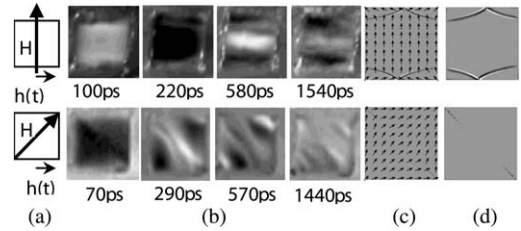


Fig. 3. (a) Experimental geometries and (b) dynamic Kerr images at four time delays are shown. (c) Simulated static magnetic images ( $M_Z$ ) and (d) internal field ( $H_{\text{int}(z)}$ ) distributions are shown.

Dynamic magnetic images were acquired to elucidate the variations in the apparent damping. Fig. 3(a) shows the two configurations ( $\phi_H = 0^\circ$  and  $45^\circ$ ) used. Fig. 3(b) shows images at four different delay times. The non-uniformity develops from the edge regions perpendicular to  $\mathbf{H}$  for  $\phi_H = 0^\circ$  and from the central region of the element for  $\phi_H = 45^\circ$ . Consequently, dephasing at the position of the probe spot occurs more quickly for  $\phi_H = 45^\circ$  than for  $\phi_H = 0^\circ$ . The dominance of the lower frequency mode for  $\phi_H$  close to  $45^\circ$  in Fig. 1(c) also supports this observation. Simulated images of  $M_Z$  and the out of plane component of the total internal field  $H_{\text{int}(z)}$  in the static configuration are shown in Figs. 3(c) and (d). They show that  $M_Z$  and  $H_{\text{int}(z)}$  are non-uniform in the regions from which the non-uniformity spreads. This indicates that the sample shape has a major influence in determining the spatial variation of the static magnetisation, which affects the precession of the magnetisation.

In conclusion, we observed a four-fold variation of the damping and precession frequency in a square element of  $10 \mu\text{m}$  length by TRSKEM. Dynamic images and micromagnetic simulations were used to understand this behaviour. As  $\phi_H$  varies from  $0^\circ$  to  $45^\circ$ , regions of non-uniform magnetisation move from near the edge of the element to its centre, causing the internal field and precession frequency to vary. The non-uniformity that develops from the demagnetised regions leads to the observed variation of the damping.

We gratefully acknowledge the financial support of the EPSRC.

## References

- [1] W.K. Hiebert, et al., Phys. Rev. Lett. 79 (1997) 1134.
- [2] Y. Acremann, et al., Science 290 (2000) 492.
- [3] A. Barman, et al., Appl. Phys. Lett. 82 (2003) 3065.
- [4] S.M. Cherif, et al., J. Magn. Magn. Mater. 242–245 (2002) 591.
- [5] R.P. Cowburn, et al., Phys. Rev. Lett. 81 (1998) 5414.
- [6] L.D. Landau, et al., Phys. Z. Sowjetunion 8 (1935) 153.
- [7] M. Donahue, et al., URL <http://math.nist.gov/oommf>.